Second Order Sliding Mode Control Using Homogeneity Approach to Control a Fixed-Wing UAV

Lamia Melkou*, Mustapha Hamerlain

Robotique & Productique, Centre de Développement des Technologies Avancées – CDTA, PO, Box 17 Baba-Hassen, Algiers 16303, Algeria.

* Corresponding author. Tel.: +213550217668; email: lmelkou@yahoo.fr
Manuscript submitted June 18, 2018; accepted August 14, 2018.
doi: 10.17706/ijcee.2019.11.1.70-77

Abstract: The purpose of this paper consists of developing a robust control law for a fixed wing Unmanned Aerial Vehicle (UAV). To reach such a goal, a homogeneous continuous super twisting algorithm is used to solve the problem of attitude control for an aircraft model known by its nonlinearity and its strong coupling. Being a class of high order sliding mode (HOSM) control, super twisting algorithm (STW) allows finite time output convergence and chattering minimization for systems having relative degree equal to one. Hence, the use of homogeneity that allows the implementation of HOSM to control systems that have relative degree greater than one. Simulation results are shown to demonstrate the robustness of the proposed controller.

Key words: Fixed-wing UAVs, homogeneous control, sliding mode control law, super twisting, stabilization.

1. Introduction

In recent years, UAVs present a major interest in many technological areas. The use and development of these engines attract increasingly researchers and engineers due to their important applications such as traffic controls, aerial search, exploration of disasters, etc. Among the various types of UAVs, aircrafts (with fixed wings) are known for their remarkable advantages such as: longer flight autonomy, larger areas covered in less time, higher flight safety, etc. [1]. However, aircraft flight control design is highly challenging because of dynamics complexity and system coupling. For these reasons, UAV's modeling has been more developed, though real systems can be represented by approximate models because of aerodynamic effects [2].

Wherefore, it is advisable to use robust control algorithms to deal with cited problems. Several approaches have been proposed such as: fuzzy control [3], nonlinear $H\infty$ state feedback [4], neural control [5], nonlinear control [6], etc.

Variable structure control algorithm generating sliding mode (SM) is well-known contol law. This approach is reputed by its effectiveness to control dynamic systems, notably HOSMs [7], [8] which ensure a finite time convergence and reduce chattering which is the principal inconvenient of the SM controllers [9], [10]. In aircraft control, most of the works that use HOSM focus on the Second Order Sliding Mode (SOSM) [11], [12]. Among them, we cite STW algorithm that is reputed for its robustness and finite time convergence [13]. Besides the benefits of HOSM, the STW implementation doesn't request the definition of the sliding variable time derivative [14]. STW is applied on systems that have relative degree equal to one. The homogeneity approach is used to establish its finite time convergence [15]. Recently, modified super twisting algorithm

destinated to systems having dimension greater than one has been developed in [16]. In order to constrain all model states to converge to their initial values in a finite time, the modified super twisting algorithm has been improved in [17].

In this work, aircraft attitude is controlled by the use of a homogeneous super twisting-like continuous control algorithm.

Organization of the paper is as following. In section two, the airplane is represented by its nonlinear mathematical model. In section three, homogeneous super twisting-like continuous controller is designed to control aircraft attitude. In section four, simulation results are illustrated. Finally, the paper is concluded with some remarks and future work in section five.

2. Aircraft Modeling

The aircraft used in this work is "Ultra stick 25E" [18]. The mathematical equations of its nonlinear model are detailed in [19]. The aircraft can be represented in the reference trihedron presented in Fig. 1:

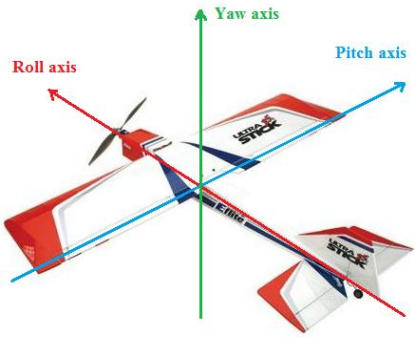

Fig. 1. Aeronautical axis conventions.

- The x-axis: longitudinal axis or roll axis.
- The y-axis: transverse axis or pitch axis.
- The z-axis: yaw axis.

These movements are generated by the control surfaces: rudder (δr), elevator (δe) and ailerons (δa) that are presented in Fig. 2.

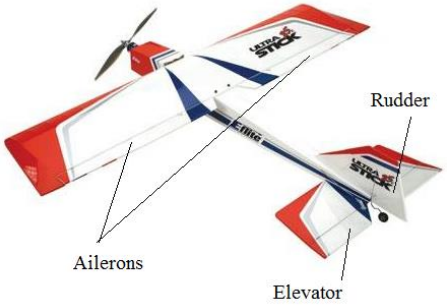

Fig. 2. Aircraft control surfaces.

The state variables are presented by the vector $X = \left[U\ V\ W\ P\ Q\ R\ \phi\ \theta\ \psi\ h\right]^T$. Where: "$U$, V and W" represent the linear velocities. "P, Q and R" represent the angular rates. "ϕ, θ and ψ" Euler angles that describe the attitude of the aircraft. And "h" is the altitude.

In this work we deal with attitude control, so the state variables used are Euler angles.

Let us define $X = \begin{bmatrix} x_1 & x_2 \end{bmatrix}^T$ the new state vector.

With $x_1 = \begin{bmatrix} \theta & \phi & \psi \end{bmatrix}^T$; $x_2 = \dot{x}_1$ such as.

$$\dot{x}_1 = \begin{bmatrix} \dot{\theta} \\ \dot{\phi} \\ \dot{\psi} \end{bmatrix} = \begin{bmatrix} P + tan\theta(Qsin\phi + Rcos\phi) \\ Qcos\phi - Rsin\phi \\ (Qsin\phi + Rcos\phi)/cos\theta \end{bmatrix} \tag{1}$$

It is noticed that the control variables do not appear explicitly in (1). So, equation (1) should be derived.

$$\dot{x}_2 = \begin{bmatrix} \ddot{\theta} \\ \ddot{\phi} \\ \ddot{\psi} \end{bmatrix} = \begin{bmatrix} A_{11} \\ B_{11} \\ C_{11} \end{bmatrix} + \begin{bmatrix} Ae & Aa & Ar \\ Be & Ba & Br \\ Ce & Ca & Cr \end{bmatrix} * \begin{bmatrix} \delta e \\ \delta a \\ \delta r \end{bmatrix} \tag{2}$$

These variables are presented in the appendix. The next step consists of defining the control law to stabilize this multivariable system of dimension 2.

3. Control Design

In this section we develop a controller that uses homogeneous super twisting-like continuous control algorithm providing the attitude aircraft control and stabilization. For this, let us consider the double-integrator nonlinear system of dimension two:

$$\begin{cases} \dot{x}_1 = x_2 & x_1(t_0) = x_{10} \\ \dot{x}_2 = f(x) + g(x)u & x_2(t_0) = x_{20} \end{cases} \tag{3}$$

$u(t) = \begin{bmatrix} \delta e & \delta a & \delta r \end{bmatrix}^T$ represents the vector input.

The super twisting algorithm presented by "(4)" is used to design a continuous finite-time stabilizing control for systems with relative degree $r = 1$ [20].

$$u(t) = -\lambda \left| x(t) \right|^{1/2} \operatorname{sgn}\left(x(t) \right) - \alpha \int_{t_0}^{t} \operatorname{sgn}\left(x(s) \right) ds \tag{4}$$

With $\lambda, \alpha \succ 0$.

For $r = 2$, Twisting control law is used to ensure finite time system stabilization [21]:

$$u(t) = -k_1 \operatorname{sgn}\left(x_1(t) \right) - k_2 \operatorname{sgn}\left(x_2(t) \right), \qquad k_1, k_2 \succ 0 \tag{5}$$

The homogeneous super twisting-like continuous modification of the twisting control law (6) given by [17] is used to control a system of dimension two.

$$u(t) = -\lambda_0 \left| \int_{t_0}^{t} x_1(s) ds \right|^{1/4} \operatorname{sgn}\left(\int_{t_0}^{t} x_1(s) ds \right) - \lambda_1 \left| x_1(t) \right|^{1/3} \operatorname{sgn}\left(x_1(t) \right) - \lambda_2 \left| x_2(t) \right|^{1/2} \operatorname{sgn}\left(x_2(t) \right) - \alpha \int_{t_0}^{t} \operatorname{sgn} x_2(s) ds \tag{6}$$

With: $\lambda_0,\ \lambda_1,\ \lambda_2,\ \alpha \succ 0$.

This control law ensures convergence in finite-time of the states $\left(x_1(t) \right)$ and $\left(x_2(t) \right)$ of system "(3)" to the origin with degree of homogeneity equal to (-1) as in [22].

Demonstration

The system state $x(t) \in R^n$ converge to a state $x_f \in R^n$ in finite time, if there exists a time moment T such that $x(t) = x_f$ for all $t \geq T$, and this for any initial condition $x(t_0) = x_0 \in R^n$.

Lemma 1 [17]: Consider a non linear system "(3)" of dimension two. The following modified super twisting control law (7) leads to a finite-time convergence of both states $(x_1(t))$ and $(x_2(t))$ to a point $[x_{1f}, 0]$.

$$u(t) = -\lambda_1 |x_1(t)|^{1/3} \operatorname{sgn}(x_1(t)) - \lambda_2 |x_2(t)|^{1/2} \operatorname{sgn}(x_2(t)) - \alpha \int_{t_0}^{t} \operatorname{sgn} x_2(s) ds \tag{7}$$

Proof: By the use of "(3)" and "(6)" we obtain:

$$\begin{aligned} &\dot{x}_1(t) = x_2(t) && x_1(t_0) = x_{10} \\ &\dot{x}_2(t) = \lambda_1 |x_1(t)|^{1/3} \operatorname{sgn}(x_1(t)) - \lambda_2 |x_2(t)|^{1/2} \operatorname{sgn}(x_2(t)) + x_3(t) && x_2(t_0) = x_{20} \\ &\dot{x}_3(t) = -\alpha \operatorname{sgn} x_2(s) && x_3(t_0) = 0 \end{aligned} \tag{8}$$

Let us consider f the vector field obtained from the right-hand side of "(8)" such as:

$$f = g_1 + g_2$$

Where g_1 and g_2 are two homogeneous vector fields with homogeneity degrees $m_1 = m_2 = -1$.

$$g_1 = \left[x_2, -\lambda_1 |x_1(t)|^{1/3} \operatorname{sgn}(x_1(t)) - \rho\lambda_2 |x_2(t)|^{1/2} \operatorname{sgn}(x_2(t)), 0 \right], \rho \in (0,1)$$

$$g_2 = \left[0, -(1-\rho)\lambda_2 |x_2(t)|^{1/2} \operatorname{sgn}(x_2(t)) + x_3, -\alpha \operatorname{sgn} x_2(t) \right]$$

The Lyapunov function $V(x_1, x_2) = \lambda_1 (3/4) |x_1(t)|^{4/3} + (1/2) |x_2(t)|^2$ is to be considered.

By considering this Lyapunov function and g_1 homogeneity, the field g_1 ensures the finite-time stability at a point $[0, 0, x_3(t_0)]$. The field g_2 represents the super twisting algorithm, which converges to the point $[x_{1f}, 0, 0]$ in a finite time.

4. Simulation Results

In this section, simulation results are presented to show the performance of the used controller.

As mentioned above, the aircraft movement occurs by the surface deflections that represent the control signals: (δe) produces the pitch motion, (δa) the roll movement, and (δr) the yaw rotation. However, the coupling phenomenon can be noticed when observing the state equation (2). For instance, yaw and roll motions are operated simultaneously by rudder and ailerons deflections.

The simulation phase was tedious and took much time because of the coupling. Indeed, when adjusting each gain parameter the other systems responses can be affected.

Simulation results of roll and yaw movements are presented hereinafter. First, the tracking errors of the two movements are shown in Fig. 3 and Fig. 4. These movements are generated by aileron and rudder deflection (δa) and (δr) presented in Fig. 5 and Fig. 6. The sliding surfaces for these two variable states and their first derivatives are shown respectively in Fig. 7-10.

Matlab Simulink software has been used to perform different simulations. Desired values of the angles are

fixed to 0°($\phi_{des} = \psi_{des} = 0°$) to maintain a rectilinear trajectory. The sampling period is fixed to 0.01s, and simulation duration is 50 s. Obtained results are compared to those presented in [19] (red curves) where a classical super twisting STW controller has been developed.

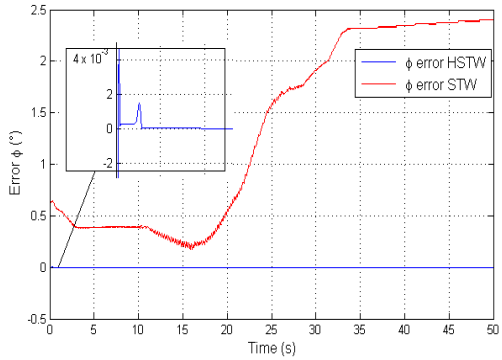

Fig. 3. Tracking error of roll angle (ϕ).

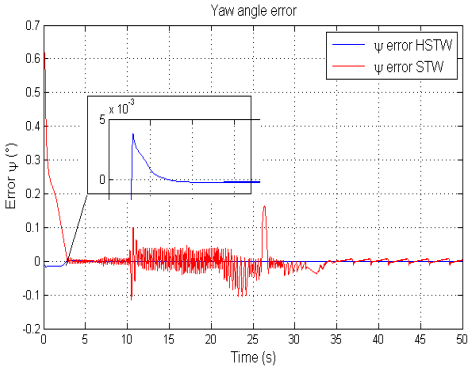

Fig. 4. Tracking error of yaw angle (ψ).

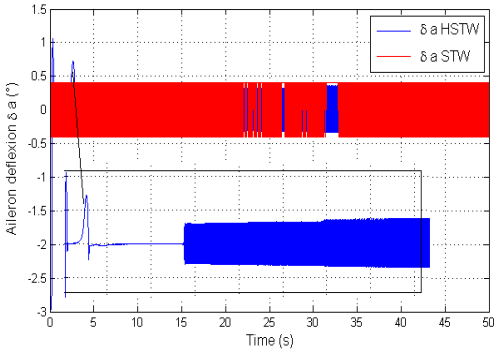

Fig. 5. Aileron deflection (δa).

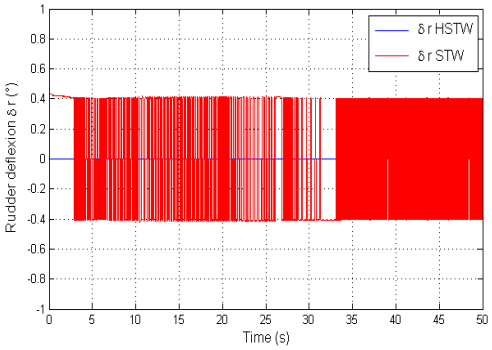

Fig. 6. Rudder deflection (δr).

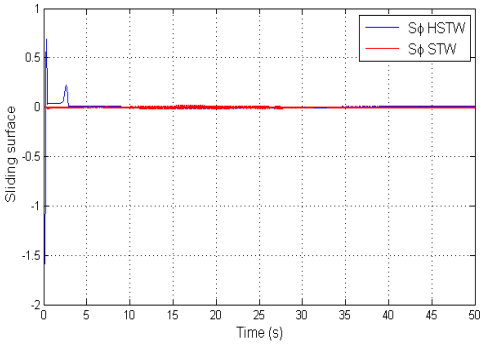

Fig. 7. Surface deflection (roll motion).

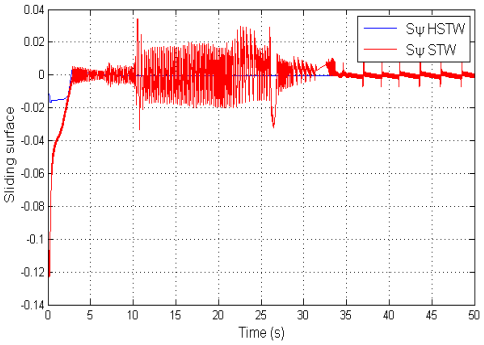

Fig. 8. Surface deflection (yaw motion).

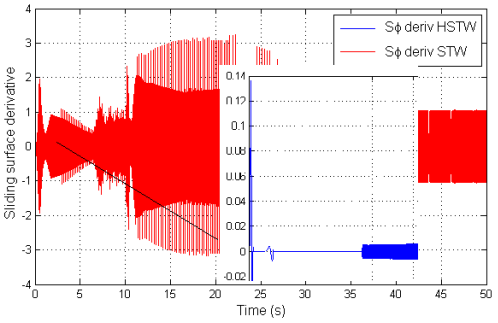

Fig. 9. Surface deflection derivative (roll motion).

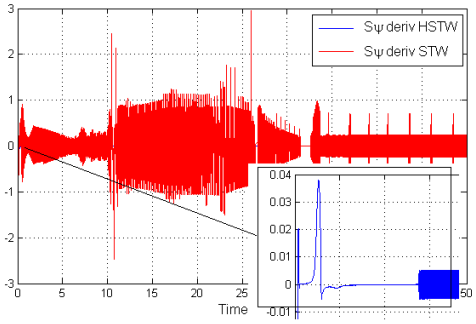

Fig. 10. Surface deflection derivative (yaw motion).

As shown in Fig. 3, the roll error is eliminated in the third second without overshoot. It does not exceed 4x10-3 degrees at the transient regime. Then it vanishes at the steady state in contrary to the STW where the static error is equal to 2 .5°. For the yaw movement, we notice the same aircraft behavior. Fig. 4 shows that the maximum value of the error does not exceed 5x10-3 degree during the first three seconds. Then, it vanishes in the 5th second. We notice that the curve is smooth compared to the STW one. From these figures, we remark that the output signals convergence to their desired values in a finite time, that confirms the high accuracy tracking trajectories of roll and yaw movements ensured by the use of HSTW.

Performances of this controller are shown in Fig. 5 and Fig. 6. The aileron deflection (δa) is measured in degrees. At the transient regime it reaches 1° then it vanishes in the fifth second. It stills at zero until t = 14s, then it starts to oscillate between -0.5 ° and + 0.5 ° throughout the rest of simulation. We notice that this command is not energetic and these weak oscillations do not affect the actuator. These oscillations are small compared to those caused by the STW algorithm.

Furthermore, it can be noticed from Fig. 6 that the rudder deflection is null during whole simulation. In fact, when adjusting the yaw gains, the best responses are obtained when these gains are null. The least value affects the other aircraft output signals. Whence, we concluded that the roll gains act also on the yaw movement, which can be explained by the strong coupling existing between different elements of the system. It is clear from this figure that the use of HSTW eliminates the chattering present in the STW.

Regarding the sliding manifolds, Fig. 7 shows that the HSTW roll sliding surface reaches 0.5 at transient regime and vanishes at steady state. The weak oscillations present in STW are eliminated. In Fig. 8 the chattering present in the STW manifold is clearly eliminated by the use of HSTW.

Curves representing the sliding surface derivative for roll movement (Fig. 9) show its convergence to zero in the HSTW mode. Small oscillations are noticed from the 14 second. They don't exceed (±0.01) in contrary to oscillations present in STW. The same remarks can be noted when observing Fig. 10 where the yaw movement sliding surface derivative is represented.

All these results show the improved performance provided by the use of HSTW. Compared to the STW, HSTW eliminates the static error present in the roll motion. It also reduces (or eliminates) the chattering caused by the STW. That confirms the effectiveness of the used controller.

5. Conclusion

This paper deals with the development of a homogeneous super twisting-like continuous modification of the twisting control law to stabilize a fixed wing UAV attitude. Aerodynamics effects, coupling and nonlinearities that characterize aircrafts make their control delicate and difficult. Hence, the need for a robust controller. The one used in this work is advised to improve the performance of the controlled system.

The use of homogeneity allowed us to exploit the advantages of HOSM to control a system with relative degree more than one. Obtained results show the efficiency of this algorithm and its robustness toward nonlinearities and coupling existing in the aircraft model.

The comparison done with obtained results by using STW [19] allowed us to conclude that the homogeneity provides remarkable improvements to the fixed wing UAV attitude control. In our future works we intend to control pitch motion and altitude.

Appendix

$$A_{11} = A + A_1 c_7 M1 + \left(A_2 c_4 + c_3\right) L_1 + \left(A_2 c_9 + c_4\right) N_1$$

$$A = (Q\cos\phi - R\sin\phi)(Q\sin\phi + R\cos\phi) / \cos^2\theta + \tan\theta(Q\cos\phi - R\sin\phi)(P + \tan\theta(Q\sin\phi + R\cos\phi)) + (c_1 R + c_2 P)Q +$$

$$\tan\theta\sin\phi(c_5 PR - c_6(P^2 - R^2)) + \tan\theta\cos\phi(c_8 P - c_2 R)Q$$

$A_1 = tan\theta sin\phi \qquad A_2 = tan\theta cos\phi$

$M_1 = qSc(cm0 + cm\alpha * \alpha + (c/2Va)(cm\dot{\alpha} * \dot{\alpha} + cmq * Q))$

$L_1 = qSb(cl\beta * \beta + (b/2Va)(clp * P + clr * R)) \qquad N_1 = qSb(cn\beta * \beta + (b/2Va)(cnp * P + cnr * R))$

$Ae = A_1 * c7 * q * S * c * cm\delta e; \quad Aa = qSb((A_2c_4 + c_3)cl\delta a + (A_2c_9 + c_4)cn\delta a); \quad Ar = qSb((A_2c_4 + c_3)cl\delta r + (A_2c_9 + c_4)cn\delta r).$

$B_{11} = B + cos\phi c_7 M_1 - sin\phi c_4 L_1 - sin\phi c_9 N_1$

$B = -(Qsin\phi + Rcos\phi)(P + tan\theta(Qsin\phi + Rcos\phi)) + cos\phi(c_5 PR - c_6(P^2 - R^2)) - sin\phi(c_8 P - c_2 R)Q$

$Be = cos\phi c_7 qSc.cm\delta e; \; Ba = -qSbsin\phi(c_4 cl\delta a + c_9 cn\delta a); \; Br = -qSbsin\phi(c_4 cl\delta r + c_9 cn\delta r).$

$C_{11} = C + C_1 c_7 M_1 + C_2 c_4 L_1 + C_2 c_9 N_1$

$C = (sin\theta sin\phi / cos^2\theta + cos\phi / cos\theta)\dot{\phi}Q + (sin\theta cos\phi / cos^2\theta - sin\phi / cos\theta)\dot{\phi}R + (sin\phi / cos\theta)(c_5 PR - c_6(P^2 - R^2)) + (cos\phi / cos\theta)(c_8 P - c_2 R)Q$

$C_1 = sin\phi / cos\theta; \; C_2 = cos\phi / cos\theta; \; Ce = C_1 c_7 qSc.cm\delta e; \; Ca = C_2 qSb(c_4 cl\delta a + c_9 cn\delta a); \; Cr = C_2 qSb(c_4 cl\delta r + c_9 cn\delta r).$

The values of constants c_1 to c_9 are obtained in terms of the airplane moment inertia coefficients. All parameters and coefficients are given in [19].

References

[1] Vantaggi degli UAV ad ala fissa rispetto a quelli ad ala rotante. Retrieved from http://www.cleverdronemaps.com/advantages-of-fixed-wing-uav-than-rotary-wing

[2] Stevens, B. L., Lewis, F. L., & Johnson, E. N. (2015). Aircraft control and simulation: Dynamics, controls design, and autonomous systems. John Wiley & Sons.

[3] Cervantes, L., & Castillo, O. (2015). Type-2 fuzzy logic aggregation of multiple fuzzy controllers for airplane flight control. *Information Sciences, 324*, 247-256.

[4] Ferreira, H. C., Baptista, R. S., Ishihara, J. Y., & Borges, G. A. (2011, December). Disturbance rejection in a fixed wing UAV using nonlinear H∞ state feedback. *Proceedings of the 2011 9th IEEE International Conference on Control and Automation (ICCA)* (pp. 386-391).

[5] Ambati, P. R., & Padhi, R. (2017). Robust auto-landing of fixed-wing UAVs using neuro-adaptive design. *Control Engineering Practice, 60*, 218-232.

[6] Xu, B., Wang, S., Gao, D., Zhang, Y., & Shi, Z. (2014). Command filter based robust nonlinear control of hypersonic aircraft with magnitude constraints on states and actuators. *Journal of Intelligent & Robotic Systems, 73(1-4)*, 233-247.

[7] Orra, J., & Shtessel, Y. (2010). Lunar spacecraft powered descent control using higher-order sliding mode techniques. *Journal of the Franklin Institute, 34,* 476-492.

[8] Pukdeboon, C., Zinober, A. S., & Thein, M. W. L. (2010). Quasi-continuous higher order sliding-mode controllers for spacecraft-attitude-tracking maneuvers. *IEEE Transactions on Industrial Electronics, 57(4)*, 1436-1444.

[9] Wang, J., Zong, Q., Su, R., & Tian, B. (2014). Continuous high order sliding mode controller design for a flexible air-breathing hypersonic vehicle. *ISA transactions, 53(3)*, 690-698.

[10] Yamasaki, T., Balakrishnan, S. N., & Takano, H. (2012). Integrated guidance and autopilot design for a chasing UAV via high-order sliding modes. *Journal of the Franklin Institute, 349(2)*, 531-558.

[11] Levant, A., Pridor, A., Gitizadeh, R., Yaesh, I., & Ben-Asher, J. Z. (2000). Aircraft pitch control via second-order sliding technique. *Journal of Guidance, Control, and Dynamics, 23(4)*, 586-594.

[12] Ali, S. U., Samar, R., Shah, M. Z., Bhatti, A. I., Munawar, K., & Al-Sggaf, U. M. (2016). Lateral guidance and

control of UAVs using second-order sliding modes. *Aerospace Science and Technology, 49*, 88-100.

[13] Kochalummoottil, J., Shtessel, Y. B., Moreno, J. A., & Fridman, L. (2012, June). Output feedback adaptive twisting control: A Lyapunov design. *Proceedings of the American Control Conference (ACC)* (pp. 6172-6177). IEEE.

[14] Rivera, J., Garcia, L., Mora, C., & Ortega, S. (2011). Super-twisting sliding mode in motion control systems. *Sliding mode control. InTech*.

[15] Bhat, S. P., & Bernstein, D. S. (2005). Geometric homogeneity with applications to finite-time stability. *Mathematics of Control, Signals and Systems, 17(2)*, 101-127.

[16] Basin, M., & Rodriguez-Ramirez, P. (2014, June). A modified super-twisting algorithm for systems of relative degree more than one. *Proceedings of the 2014 13th International Workshop on Variable Structure Systems (VSS)* (pp. 1-6). IEEE.

[17] Basin, M. V., & Ramírez, P. C. R. (2014). A supertwisting algorithm for systems of dimension more than one. *IEEE Transactions on Industrial Electronics, 61(11)*, 6472-6480.

[18] Paw, Y. C., & Balas, G. J. (2011). Development and application of an integrated framework for small UAV flight control development. *Mechatronics, 21(5)*, 789-802.

[19] Melkou, L., Hamerlain, M., & Rezoug, A. (2017). Fixed-wing UAV attitude and altitude control via adaptive second-order sliding mode. *Arabian Journal for Science and Engineering*, 1-12.

[20] Moreno, J. A., & Osorio, M. (2012). Strict Lyapunov functions for the super-twisting algorithm. *IEEE transactions on automatic control, 57(4)*, 1035-1040.

[21] Levant, A., Taleb, M., & Plestan, F. (2011, December). Twisting-controller gain adaptation. *Proceedings of the 2011 50th IEEE Conference on Decision and Control and European Control Conference (CDC-ECC)* (pp. 7015-7020). IEEE.

[22] Levant, A. (2005). Homogeneity approach to high-order sliding mode design. *Automatica, 41(5)*, 823-830.

Melkou Lamia received the doctorate degree in 2018 from University of Annaba, Algeria. She is a researcher in the Robotics and Automation Department of the Advanced Technologies and Development Center (CDTA) of Algiers. She has worked on microcontrollers and smart card programming. In 2011 she obtained a master degree in automation. Currently, her research activities deal with the robust control and modeling of dynamic systems.

Hamerlain Mustapha is a research director; he received the doctorate degree in 1993 from National Institute of Applied Sciences of Toulouse (France). He is a researcher in the Robotics Department of the Advanced Technologies and Development Center (CDTA) of Algiers and a professor at the school (EMP). From 1988 to 1993 he was involved in a research project in the field of robotics PAM (Pneumatic Artificial Muscles) as a researcher in the National Institute of Applied Sciences (INSA) of Toulouse. His current research interests include robust control of nonlinear systems, robot motion control, visual control, robots manipulators and pneumatic artificial muscles actuators.